The 9th International Symposium on NDT in Aerospace
8-10 November, 2017, Xiamen, China

Damage assessment in composite materials using full wavefield analysis

Tomasz WANDOWSKI[1], Pawel H. MALINOWSKI[1],
Wieslaw M. OSTACHOWICZ[1,2]

[1]Institute of Fluid Flow Machinery, Polish Academy of Sciences, Gdansk, Poland
[2]Faculty of Automotive and Construction Machinery, Warsaw University of Technology, Warsaw, Poland
Corresponding author: Tomasz Wandowski, e-mail: tomaszw@imp.gda.pl

Abstract
In this paper damage assessment method is presented. This method is based on phenomenon of guided elastic waves propagation. Guided waves are generated by piezoelectric transducer and registered by Scanning Laser Doppler Vibrometer (SLDV). Signal processing is based on the analysis of full wave-field measurements. In this approach guided wave signals are gathered from dense mesh of measurement points spanned over investigated area of investigated structure. This approach allows to create animations representing the guided wave propagation which are suitable for analysis of interaction of guided waves with different discontinuities located in composite material. In the research attention is especially focused on analysis of phenomenon of guided wave mode conversion. This phenomenon occurs due to the interaction of guided wave with discontinuities in the structure. Guided wave mode conversion phenomenon has potential for damage detection. Method is validated for the fibre reinforced composite materials. In the research such discontinuities like delamination simulated by teflon insert with different shapes and location as well as true delamination created by impact are investigated.
In the research auxiliary nondestructive testing (NDT) method is utilized. The aim of this method is to indicate the depth of discontinuity, and to prove that delamination was created. Auxiliary method is based on terahertz spectroscopy (THz). This method is based on analysis of propagation of electromagnetic waves in the terahertz band. THz spectroscopy method can be utilized for damage assessment in the materials that do not conduct electric current.

Keywords: Damage assessment, Guided wave propagation (GW), Mode conversion, Terahertz spectroscopy

1. Introduction

Composite structures are more and more utilized in different branches of industry. Nowadays structures are made out of various composite materials like glass/carbon fiber reinforced polymers (GFRPs, CFRPs) or glass laminate aluminum reinforced epoxy (GLARE). Due to this fact the up-to-date NDT techniques should handle with the wide range of these materials and potential defect types that could occur in such materials. Typical damage that can initiate in composite are matrix cracking and delamination cause by impact [1],[2] but attention should be also focused on such problems like the performance of structural bonds, moisture content or thermal degradation.
There are many non-destructive testing NDT techniques that can be utilized for damage detection and localization in fibre reinforced polymers FRPs. In this purpose NDT techniques like ultrasound testing UT 1, active infrared thermography 2, eddy currents 3, X-ray tomography 4, terahertz spectroscopy 1,5 and guided waves based 6 are utilized.
In this paper results of research related to guided wave propagation method were presented. Authors also presented results of application of auxiliary NDT method based on terahertz THz spectroscopy. The aim of application of THz spectroscopy was to indicate depth of discontinuity, and to prove that delamination was created.
Guided wave propagation method can be used in Structural Health Monitoring SHM when piezoelectric transducers are utilized for elastic wave generation and sensing purposes. This method could be used also utilized as NDT technique when non-contact measurements are conducted using laser scanning vibrometer and the guided wave excitation is realized using piezoelectric transducer.

In this paper authors utilized NDT approach based on analysis of full wavefield registered by Scanning Laser Doppler vibrometry SLDV. Authors focused attention on interactions of elastic waves with discontinuities in the form of simulated delamination (teflon insert) and impact induced delamination. Attention is focused especially on guided wave mode conversion S0/A0'. Full wavefield measurement approach based on SLDV allows to visualize and analyse guided wave propagation in complex structures. Beside this, detailed analysis of GW propagation in frequency-wavenumber domain in the purpose of damage detection can be performed 6. In the papers 7, 8 damage detection approach based on local wavenumber analysis was proposed. Problem of delamination localization using full wavefield approach was for example investigated in papers 8, 9. Authors of papers 10, 11, 12 focused attention on wave trapping effect in the delaminated region. SLDV technique can be also utilized for analysis of mode conversion phenomenon 13. This phenomenon was also investigated in composite structures where S0/A0' mode conversion due to interaction of S0 mode with delamination was observed 14. The authors performed numerical and experimental research. They investigated interaction of elastic waves with delaminations with different shapes and locations (planar and in the respect to the thickness). In the numerical part Spectral Element Method (SEM) was utilized. Simulations of guided wave propagation that take into account problem of mode conversion were also conducted by authors of 15 using conventional Finite Element Method. Laser vibrometry was also utilized in research related to continuous mode conversion in carbon fiber reinforced polymer (CFRP) plates. This research was begun by Willberg et al. 16. Authors observed continuous mode conversion S0/A0 in multilayer composite plate. Conversions occur continuously as result of interaction of guided waves with reinforcement in the form of twill fabric. This phenomenon was also reported in 13. Mode conversion phenomenon was also utilized for damage detection by the authors of 17. Authors utilized 3D full wavefield measurements based on scanning laser vibrometer. Mode conversion effect was utilized as a indicator of damage.
In this paper interactions of elastic guided waves with discontinuities in the form of simulated delaminations (teflon inserts) and impact damage are investigated.

2. Measurement set-up

Experimental research was related to specimen in the form of Glass Fibre Reinforced Polymer GFRP plate with dimensions 500 mm x 500 mm and thickness ~1.5 mm (**Fig. 1**). Plate consists of twelve layers of VV192T/202 IMP503 prepregs with orientations: $[0/90/0/90/0/90]_S$. At the manufacturing stage of the plate four circular teflon inserts, each with diameter 10 mm, were located between different layers of prepreg.

Fig. 1. Investigated GFRP sample with discontinuities

Planar location of teflon inserts can be noticed in **Fig. 1**. Planar location and location between layers can be seen in **Fig. 2**, where inserts are denoted as T1 – T4. After manufacturing process different cases of impact damage was made. In the first steep, four impacts at different location and with different energy were made. Location of mentioned impacts denoted as I1 – I4 can be seen in **Fig. 2**. Impact energy for each of investigated cases can be seen in Tab. 1.

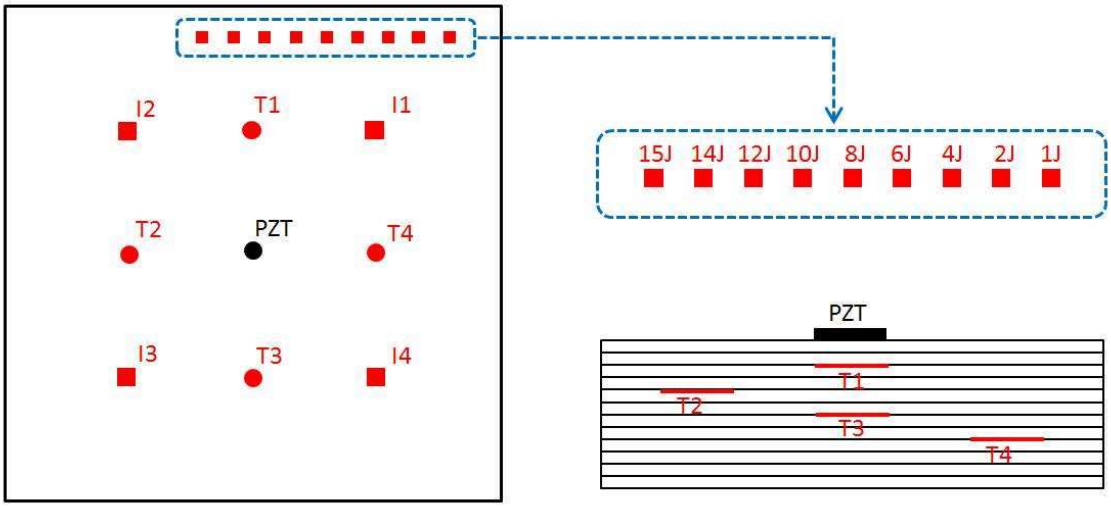

Fig. 2. Location of teflon inserts and impact damage

In next step nine additional impacts were made out near the top edge of the plate (see **Fig. 2**). In this case, impacts have different energy ranging from 1 J up to 15 J. All investigated impact energy values can be read from **Fig. 2**.

Tab. 1. Impact damage cases

Impact	Energy [J]
I1	2.5
I2	5
I3	10
I4	15

Guided waves were excited by piezoelectric transducer located in the middle of the sample, on its top surface (see Fig. 1 and Fig. 2). Guided wave sensing process was conducted using Polytec PSV-400 scanning laser vibrometer on the bottom surface of plate. Only one scanning laser head was utilized (measurements along laser beam approximating out-of-plane velocities). Measurements were performed for dense mesh of points spanned over the area of investigated GFRP plate.

3. Results for full wavefield analysis

In the Fig. 3 selected frames from animation of guided wave propagation in GFRP specimen with discontinuities mentioned in previous sections were presented. In this case excitation frequency was equal 100 kHz (tone burst excitation, 5 cycles of sine modulated by Hann window). In the Fig. 3a) propagation of two fundamental modes A0 and S0 can be noticed. Modes can be distinguished by their different wavelengths. Mode S0 has larger wavelength and higher velocity of propagation than A0 mode. In the Fig. 3a) S0 mode reflects from the plate edges.

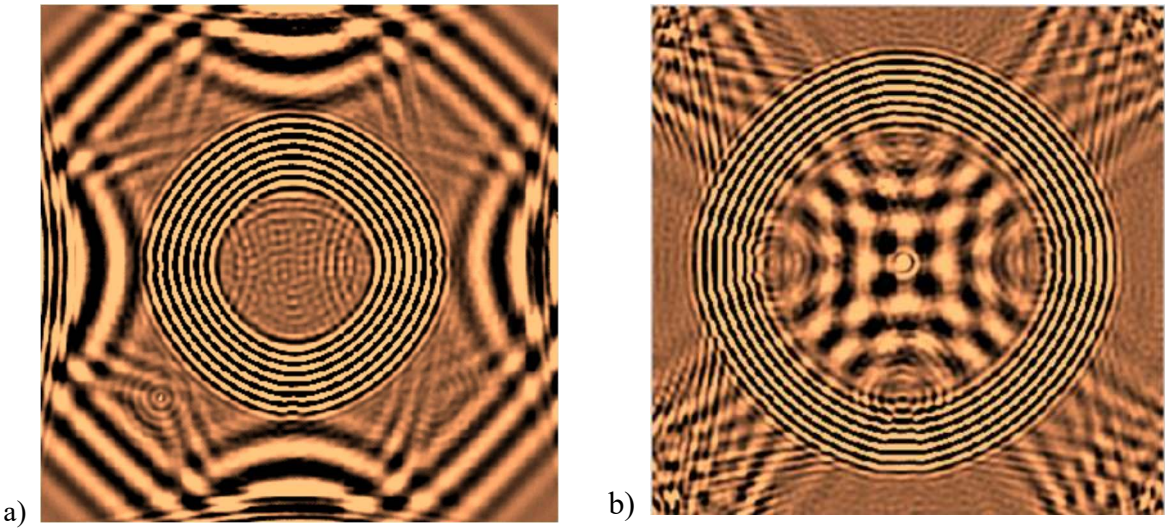

Fig. 3. Selected frames from animation of guided wave propagation in GFRP for excitation frequency 100 kHz: a, b) subsequent frames

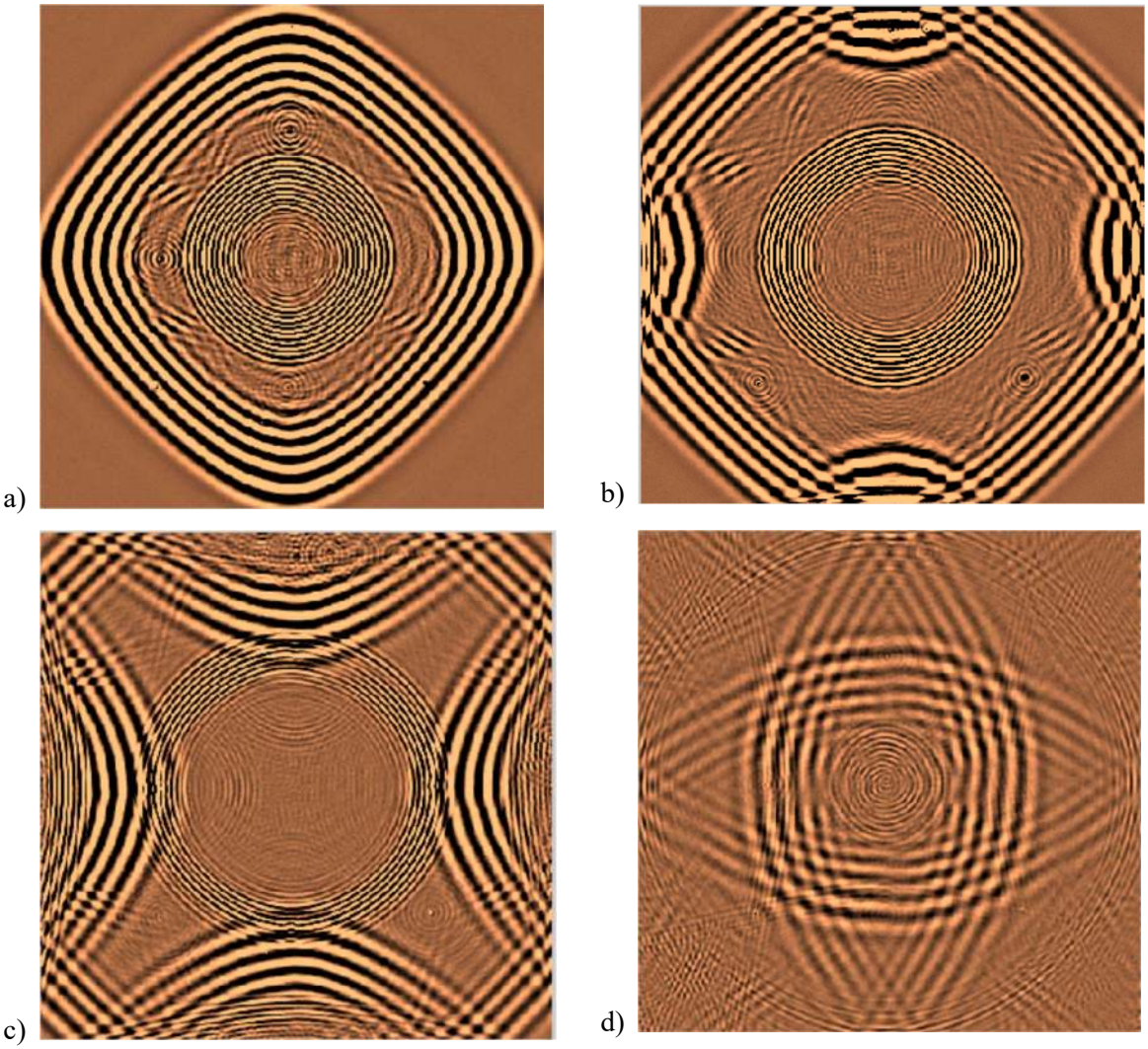

Fig. 4. Selected frames from animation of guided wave propagation in GFRP for excitation frequency 200 kHz: a-d) subsequent frames

Moreover in this figure symmetric S0 mode, due to interaction with impact damage I3 and I4 (see Fig. 2), converts to antisymmetric mode denoted as A0' (where A0' denotes antisymmetric

mode generated after S0 mode conversion). In the case of excitation frequency 100 kHz, mode conversion effect was not visible in the case of remaining discontinuities described in previous section. However, S0/A0' mode conversion phenomenon was observed on the edges of plate. Characteristic wavelength change can be observed after reflection of S0 mode from the plate edges. A0' mode with shorter wavelength propagates just after S0 edge reflected mode. This was caused by slight thickness change just near the plate edges (defects from manufacturing process). In the Fig. 3b) reflections of A0 mode from teflon inserts T1–T4 (see Fig. 2) can be seen.

In next step measurements of guided wave propagation were performed for excitation frequency equal 200 kHz. Full wavefield results in the form of subsequent frames taken from animation of guided wave propagation were presented in Fig. 4. Propagation of S0 and A0 mode is clearly visible. Frame presented in the Fig. 4a) was taken at time instant in which S0 mode reached the plate edges and already has propagated through areas with teflon inserts T1-T4. In this frame S0/A0' mode conversion resulting from interaction of S0 mode with teflon inserts can be clearly visible. What is interesting S0/A0' mode conversion occurs for teflon insert T3 which is located in the middle of plate thickness (symmetry in respect to the thickness) - Fig. 2. Mode conversion occurs in the region without symmetry. Existence of damage/discontinuity destroys the symmetry of sample and results in mode conversion 18. In the numerical results presented in 14 there was no mode conversion when the simulated delamination was located symmetrically in respect to the sample thickness. Here teflon insert T3 was located between layers sixth and seventh, in the middle of the thickness (symmetry), but mode conversion S0/A0' is clearly visible. It could be explained by the fact that in real conditions any kind of introduced discontinuity always destroy the symmetry.

In next frame (Fig. 4b) S0 mode reflects from the plate edges. Moreover S0/A0' mode conversion in the areas of impact I3 and I4 can be clearly visible. Mode conversion can be also clearly notice on the left edge of the plate. In the Fig. 4c) S0/A0' mode conversion on the all plate edges can be noticed. Moreover mode conversion is visible in the areas of impacts with energies 1 J – 15 J, near the top edge of the plate (compare with Fig. 2). Teflon inserts caused also reflections of A0 mode, that are visible in the same figure. In the last frame (Fig. 4d) S0/A0' mode conversion on the piezoelectric transducer placed in the middle of the plate. Piezoelectric transducer is a source of non symmetry for the propagating waves and therefore causes mode conversion.

4. Weighted RMS energy maps

In this section guided wave signal processing algorithm is presented which aim it to visualize discontinuities location. Algorithm is based on calculation of weighted Root Mean Square (WRMS) indicator for full wavefield measurements of guided wave propagation.

As consequence application of WRMS algorithm, energy distribution related to propagation of waves and its interaction with discontinuities in the structure is obtained. In the WRMS algorithm weight factor is utilized for the aim of compensation of guided wave damping in the investigated samples. The Weighted Root Mean Square (WRMS) can be calculated using formula:

$$WRMS = \sqrt{\frac{1}{N}\sum_{k=1}^{N} w_k s^2} \tag{1}$$

where: k - is sample number and the weighting factor w_k is defined as follows:

$$w_k = k^m, \quad m \geq 0 \tag{2}$$

In the Fig. 5 WRMS energy maps for guided wave propagation for excitation frequency 100 kHz were presented. In the Fig. 5a) WRMS energy map for the coefficient m=0.05 was presented. In this map, location of point of guided wave generation (in the middle) with the largest energy concentration is visible. Moreover locations of teflon inserts T1–T4 and impact damage I3 and I4 are clearly visible as the areas where the change of energy distribution occurs. This map does not indicate location of impacts I1 and I2 as well as impact near the top edge of plate. WRMS energy map presented in the Fig. 5b) was created for the coefficient m=0.75. In this case stronger changes in guided wave energy distribution in locations of teflon inserts T1-T4 and impact damage I3 – I4 are visible. However, energy map does not indicate locations of impacts I1 and I2 as well as impact near the edge.

a)

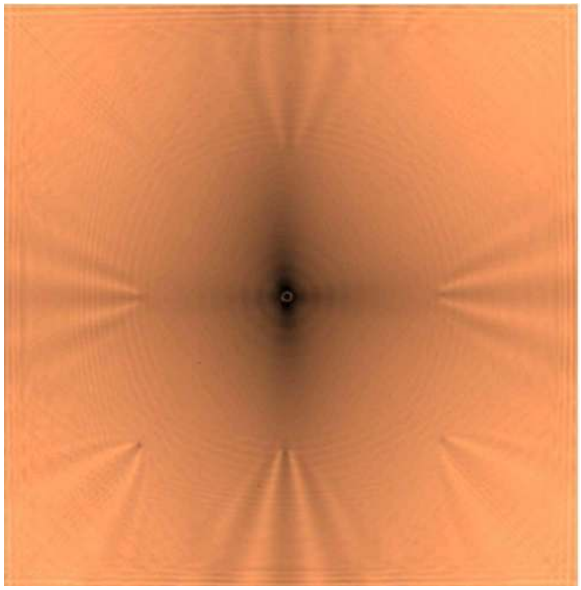

b)

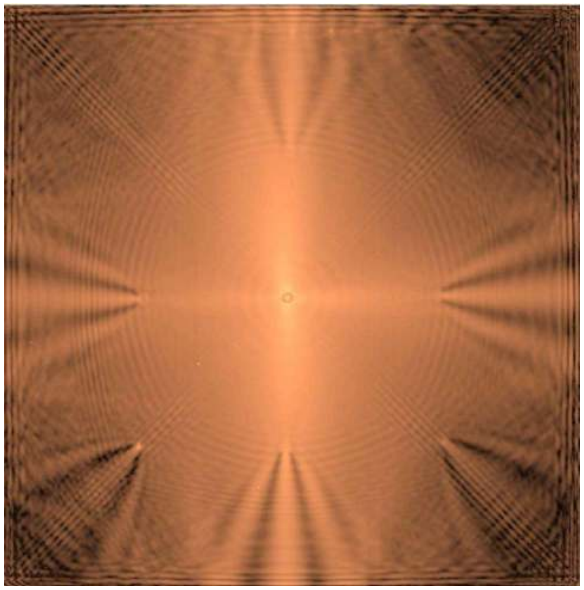

Fig. 5. WRMS energy map for excitation frequency 100 kHz: a) m=0.05, b) m=0.75

a)

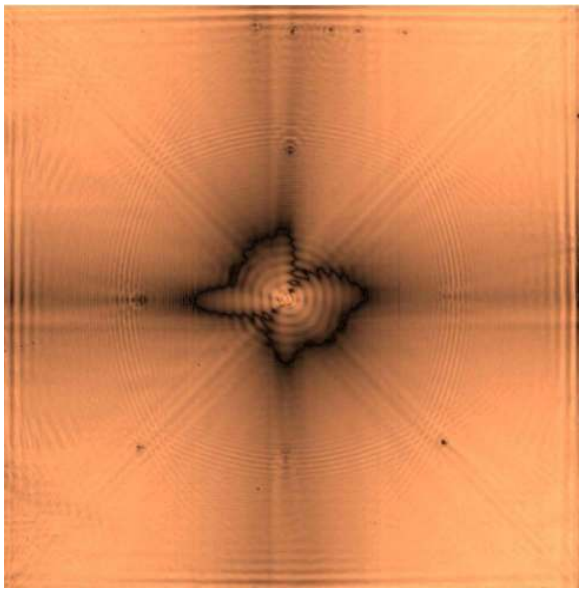

b)

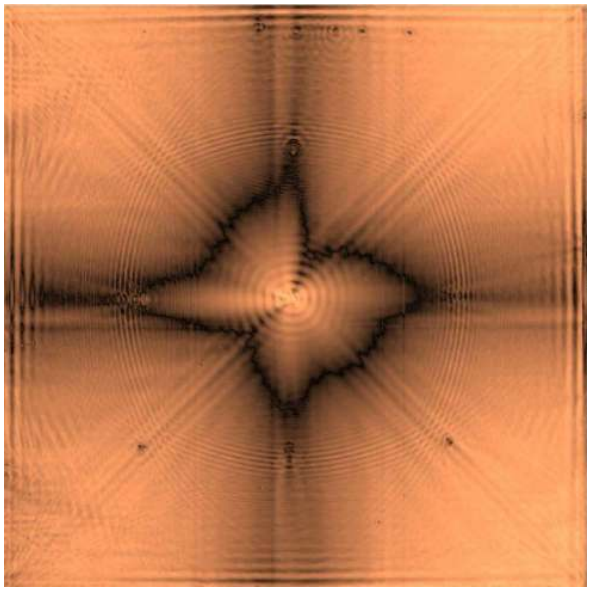

Fig. 6. WRMS energy map for excitation frequency 200 kHz: a) m=0.75, b) m=0.85

In next step WRMS energy maps for the excitation frequency 200 kHz were created.
In the Fig. 6a) WRMS energy map for the coefficient *m*=0.75 was presented. In this case point of guided wave generation (in the middle) with the largest energy concentration is visible. It should be noticed that in this area S0/A0' mode conversion on piezoelectric transducer occurs. This effect has also influence on distribution of guided wave energy. Moreover locations of four teflon inserts T1-T4 as well as impacts I3 and I4 are clearly visible. Intensity of elastic wave energy due to interaction of waves with teflon inserts depends on its location in respect to the depth of plate. Beside this, locations of impact damage, located near the top edges, are visible. Five locations of impacts with energies 15J, 14J, 12J, 10J, 8J (counting from the left to the right compare) near the top edge of plate (see Fig. 1 and Fig. 2) can be distinguished. In the Fig. 6b) WRMS energy map for the coefficient *m*=0.85 was presented. Slight change of value of coeeficient *m* improved indications of location of mentioned discontinuities. This coefficient could be used for the control of the contrast of energy map.

5. Terahertz spectroscopy

In this section results from terahertz spectroscopy are presented. Measurements were conducted using Teraview TPS Spectra 3000 spectrometer which generates impulses of electromagnetic wave in frequency range from 0.1 up to 3 THz. Impulses are sent repeatedly and interact with the investigated GFRP material and discontinuities inside (teflon inserts and impact damage). This is non-contact measurement system which allows to perform measurements in reflection and transmission modes. Results presented in this paper were based on measurements done for the scanning heads working in reflection mode. Reflection mode is more feasible for analyzing real structures where access to the structure is very often limited to only one side. The spectrometer is equipped with moving table that allows for XY scanning of large objects.
Terahertz spectroscopy is based on analysis of propagation of electromagnetic waves in the terahertz band. In the THz spectroscopy very important are differences of value of real part of refractive indexes n of interfaces of material and defect. Electromagnetic wave propagating in the material is reflected from interfaces with different values refractive indexes n. Imaginary part of refractive index is related to electromagnetic wave attenuation. THz spectroscopy method can be utilized for damage assessment in the materials that do not conduct electric current, like GFRP investigated hear. More information about method could be found in 1, 5, 19, 20.
As result of the THz spectroscopy measurement, three types of data are obtained: single signal in one point (A-scan), set of signals along line (B-scan) and set of signals in certain area (C-scan). B-scan allows to investigate the material structure in vertical cross-section (e.g.: location of defect along the thickness, determination of defect thickness and length). C-scan shows the horizontal cross-section of material at certain depth (e.g.: planar location of defects, its length and width, shape of defect).

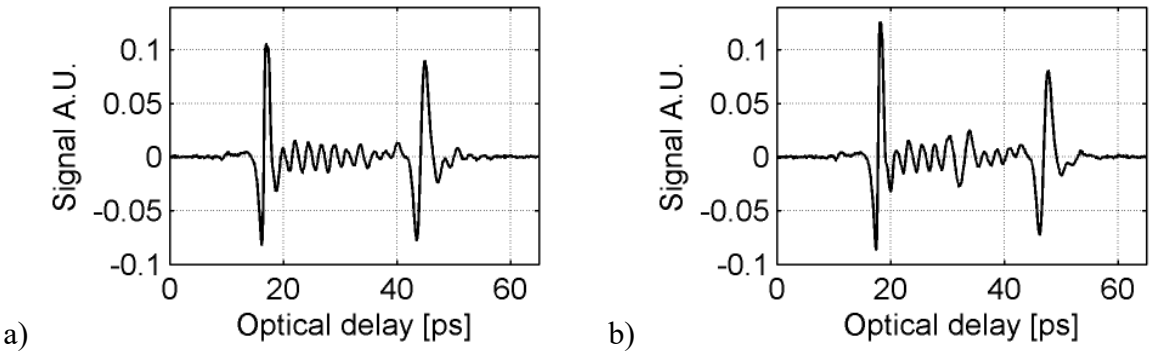

Fig. 7. THz Signals (A-scans) for GFRP sample: a) referential, b) material with teflon insert

In the Fig. 7 example of THz signals called A-scans are presented. Signal in the Fig. 7a) was created for the referential area of GFRP sample (without any defect). We can distinguish two strong reflections of electromagnetic wave: from the top surface of the sample (interface air/GFRP material) at time ~18 ps and from the bottom surface of sample (interface GFRP/air) at ~42 ps. Small reflections visible between two large peaks are related to reflection of terahertz wave at composite layers interfaces. Signal in the Fig. 7b) was taken at area of GFRP sample including teflon insert. Beside of two reflections from top and bottom surface of the sample additional reflection from the teflon insert could be noticed at ~30 ps.
This reflection was caused by different values of real parts of refractive indexes n for GFRP material and teflon. In the case of GFRP material real part of refractive index n_G=2 19, while as refractive index for teflon: n_T=1.437 20.
In the Fig. 8a-c) respectively B-scans for the areas of plate around teflon inserts T2, T3 and T4 were presented. We can noticed vertical cross-section of the GFRP sample.
Clear bottom line is related to the top surface of the sample and reflection of THz wave from it,

while as the top line is related to the bottom surface of sample. Location of teflon layer at different depth is clearly visible. In the case of Fig. 8b) B-scan was created for teflon insert T3 located in the middle of plate thickness (the same number of composite layer above and below teflon). However even in this location there is clearly visible that there is no perfect symmetry in respect to the thickness. This is source of guided wave mode conversion S0/A0' visible in Fig. 4a) and discussed in section 3. Moreover layered structure of GFRP sample is clearly visible, it is possible to distinguish all layers of the sample.
In the Fig. 9a-c) B-scans for the areas of intact GFRP plate and areas of sample around impacts I3 and I4 were presented. In the case of intact sample (Fig. 9a) the top and bottom surface of sample as well as layered structure are visible. In the case of impact I3 with energy 10 J difference in certain contrast between layers are visible (almost in the middle of the sample thickness). This contrast could be related to delamination of material.

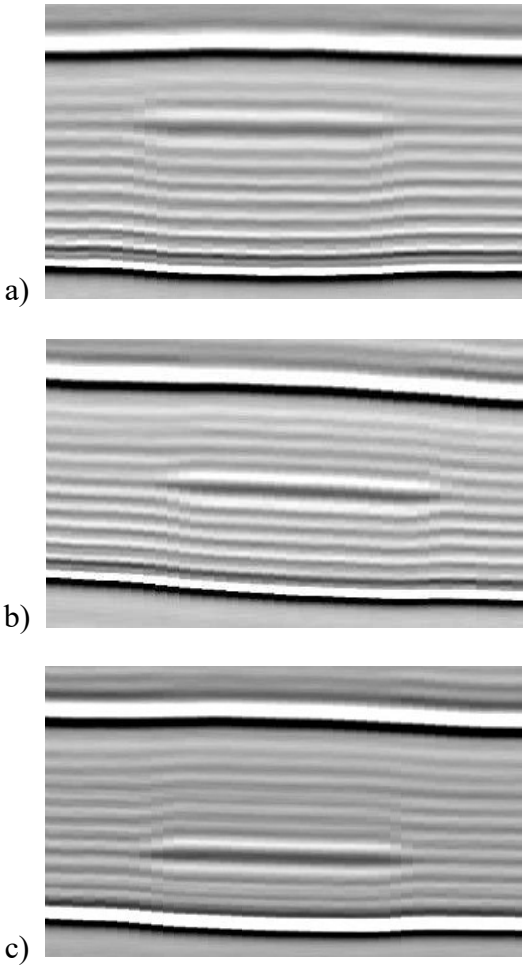

Fig. 8. B-scan for area of sample with circular teflon inserts: a) T2, b) T3, c) T4

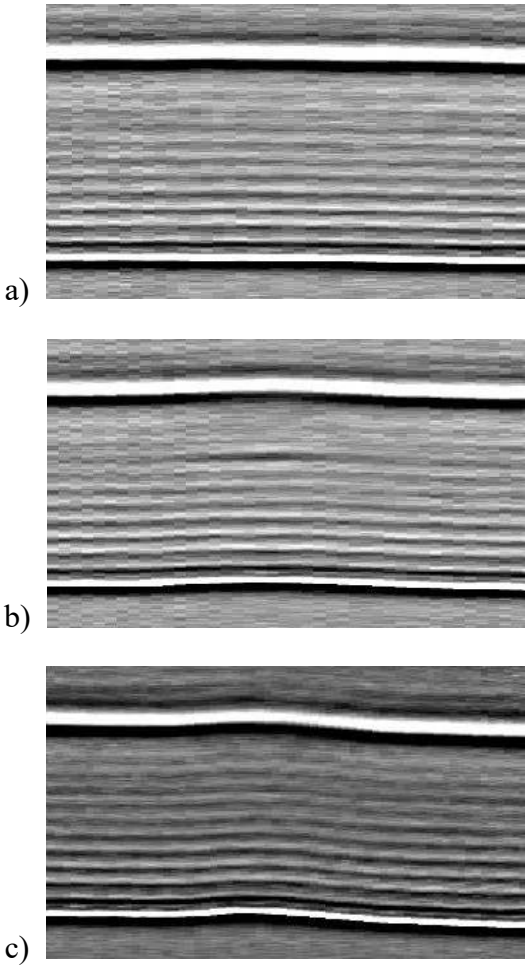

Fig. 9. B-scans for: a) referential area of sample, b) impact I3 – 10 J, c) impact I4 – 15 J

Moreover deformation of the top and bottom surface due to impact could be noticed. In the case of impact I4 with energy 15 J there is no clear contrast visible. It looks like there is no delamination. Only deformation of sample due to the impact force applied is clearly visible.
In the Fig. 10 C-scan of GFRP sample around the area where the circular teflon insert T4 was located was shown. As it was already mentioned that C-scan presents horizontal cross-section of sample. In this C-scan clear contrast between GFRP material and teflon insert is visible. Shape and diameter of insert could be determined based on C-scan.

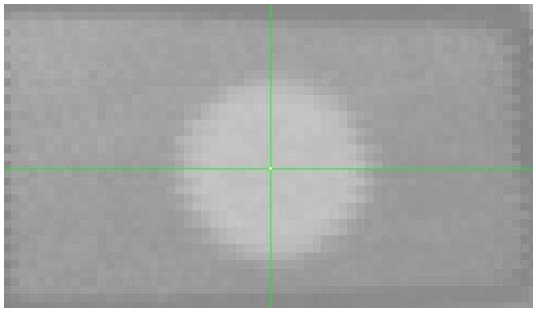

Fig. 10. C-Scan for area of GFRP sample with circular teflon insert T4

Conclusions

In this paper interactions of elastic guided waves with discontinuities in the form of simulated delaminations (teflon inserts) and impact damage were investigated. Different impact energy in the range 1 J – 15 J were investigated. In the case of teflon inserts, they have the same diameter (10 mm) but were located at different depth of plate. Teflon inserts caused S0/A0' mode conversions even in the case when inserts was located in the middle of the sample thickness (symmetry). Mode conversion S0/A0' phenomenon was observed also for the impact damage with energies 8 J – 15 J. Beside this, S0/A0' mode conversion was observed near plate edges (thickness change) and at location of piezoelectric transducer. Moreover, investigated defect caused also reflections of A0 mode.

Damage localisation algorithm based on WRMS energy of guided waves indicated location of four investigated teflon inserts T1 – T4, impact damage I3 with energy 10 J and I4 – 15 J for the excitation frequencies 100 kHz and 200 kHz. Location of impacts I1 – 2.5 J and I2 – 5 J were not indicated. In the case of excitation frequency 200 kHz also locations of additional impacts near the top plate edge (Fig. 1, Fig. 2) for the impact energies 8 J -15 J are clearly visible. Smallest energy of impact that caused structural change in the plate that can be detected by elastic waves is 8 J. Contrast of referential area to damage area in the WRMS maps can be controlled by weighting factor *m*.

Terahertz spectroscopy was utilized as auxiliary method. Aim of its application was to prove the depth at which teflon insert were located and to prove that delamination was created in the case of impact damage. THz results shows that Teflon inserts were located at correct depth according to the manufacturing specification. Moreover, even for teflon insert located in the middle of the plate thickness, there is no ideal symmetry. This fact caused A0/S0' elastic wave mode conversion. Impact force caused mainly plastic deformation of material without separation/delamination of layers. Only in the case of impact I3 with energy 10 J delamination was detected. Damage I3 with separation of layers was not indicated better than damage I4 (without delamination but with higher impact energy).

Acknowledgements

Authors would like to gratefully acknowledge financial support given by Polish National Science Centre under grant agreement no. UMO-2014/13/D/ST8/03167 in the frame of SONATA project entitled: "Investigation of elastic wave mode conversion phenomenon in thin-walled structures with discontinuities".

References

1. Dong J., Kim B., Locquet A., McKeon P., Declercq N., Citrin D.S.: *Nondestructive evaluation of forced delamination in glass fiber-reinforced composites by terahertz and ultrasonic waves.* Composites Part B, 79, 667-675, 2015.

2. Meola C., Boccardi S., Carlomagno G.M., Boffa N.D., Monaco E., Ricci F.: *Nondestructive evaluation of carbon fibre reinforced composites with infrared thermography and ultrasonic.* Composite Structures, 134, 845–853, 2015.
3. Heuer H., Schulze M., Pooch M., Gäbler S., Nocke A., Bardl G.: *Review on quality assurance along the CFRP value chain – Non-destructive testing of fabrics, preforms and CFRP by HF radio wave techniques*. Composites Part B: Engineering, 77, 494–501, 2015.
4. Uhry C., Guillet F., Duvauchelle P., Kaftandjian V.: *Optimisation of the process of X-ray tomography applied to the detection of defects in composites materials*. Proc. of. Digital Industrial Radiology and Computed Tomography (DIR 2015), Belgium, Ghent, 2015.
5. Dong J., Locquet A., Citrin D.S.: *Enhanced Terahertz imaging of small forced delamination in woven Glass Fibre-reinforced Composites with wavelet de-noising*. Journal of Infrared, Millimeter and Terahertz Waves, 37, 289–301, 2016.
6. Carrara M. and Ruzzene M.: *Frequency-wavenumber design of spiral macro fiber composite directional actuators*. Proc. of SPIE Smart Structures and Materials, 94350M-12, 2015.
7. Rogge M.D., Leckey C.A.C.: *Characterization of impact damage in composite laminates using guided wavefield imaging and local wavenumber domain analysis*. Ultrasonics, 53, 1217–1226, 2013.
8. Juarez P.D., Leckey C.A.C.: *Multi-frequency local wavenumber analysis and ply correlation of delamination damage*. Ultrasonics, 62, 56–65, 2015.
9. Murat B.I.S., Fromme P.: *Finite element modeling of guided wave scattering at delaminations in composite panels*. Proc. SPIE 9805 Health Monitoring of Structural and Biological Systems, 98050S, 2016.
10. Glushkov E., Glushakova N., Golub M.V., Moll J., Fritzen C.P.: *Wave energy trapping and localization in a plate with a delamination*. Smart Materials and Structures, 21, 125001, 2012.
11. Glushkov E.V., Glushkova N.V., Eremin A.A., Lammering R.: *Guided wave propagation and diffraction in plates with obstacles: resonance transmission and trapping mode effects*. Physics Procedia, 70, 447 – 450, 2015.
12. Tian Z., Yu L., Leckey C., Seebo J.: *Guided wave imaging for detection and evaluation of impact-induced delamination in composites*. Smart Mat Struct; Vol. 24(10), 2015.
13. Hennings B., Lammering R.: *Material modeling for the simulation of quasi-continuous mode conversion during Lamb wave propagation in CFRP-layers*. Composite Structures, http://dx.doi.org/10.1016/j.compstruct.2016.02.051, in press, 2016.
14. Wandowski T., Kudela P., Malinowski P., Ostachowicz W.: *Defect induced guided waves mode conversion*. Proc. SPIE Health Monitoring of Structural and Biological Systems 2016, Paper 9805-24, 2016.
15. Alkassar Y., Agarwal V.K. Alshrihi E.: *Simulation of Lamb wave modes conversions in a thin plate for damage detection*. Procedia Engineering 173, 948 – 955, 2017.
16. Willberg C., Koch S., Mook G., Pohl J., Gabbert U.: *Continuous mode conversion of Lamb waves in CFRP plates*. Smart Materials and Structures 21, 2012.
17. Pieczonka L., Ambrozinski L., Staszewski W.J., Barnoncel D., Peresb P.: *Damage detection in composite panels based on mode-converted Lamb waves sensed using 3D laser scanning vibrometer*. Optics and Lasers in Engineering 99, 80–87, 2017.
18. Jin J., Quek, S.T. and Wang, Q.: *Wave boundary element to study Lamb wave propagation in plates*. Journal of Sound and Vibration 288, 195–213, 2005.
19. Malinowski P., Pałka N., Opoka S., Wandowski T., Ostachowicz W.: *Moisture detection in composites by terahertz spectroscopy*. Journal of Physics: Conference Series, Volume 628, 012100, 2015.
20. Folks W.R., Pandey S.K., Boreman G.: *Refractive Index at THz Frequencies of Various Plastics*. Optical Terahertz Science and Technology 2007, Orlando, Florida United States, ISBN: 1-55752-837-3, 2007.